JACS
JOURNAL OF THE AMERICAN CHEMICAL SOCIETY
Article
pubs.acs.org/JACS

C−H Activation of Terminal Alkynes by Tris-(3,5-dimethylpyrazolyl)boraterhodiumneopentylisocyanide: New Metal−Carbon Bond Strengths

Gyeongshin Choi,[†] James Morris,[‡] William W. Brennessel,[‡] and William D. Jones*[,‡]

[†]Department of Chemistry, Graduate School of Engineering Science, Osaka University, Toyonaka, Osaka 560-8531, Japan
[‡]Department of Chemistry, University of Rochester, Rochester, New York 14627, United States

Supporting Information

ABSTRACT: C−H bond activation of terminal alkynes by [Tp′Rh(CNneopentyl)] (Tp′ = hydridotris-(3,5-dimethylpyrazolyl)borate) resulted in the formation of terminal C−H bond activation products Tp′Rh(CNneopentyl)(C≡CR)H (R = *t*-Bu, $SiMe_3$, hexyl, CF_3, *p*-$MeOC_6H_4$, Ph, and *p*-$CF_3C_6H_4$). A combination of kinetic selectivity determined in competition reactions and activation energy for reductive elimination has allowed for the calculation of relative Rh−$C_{alkynyl}$ bond strengths. The bond strengths of Rh−$C_{alkynyl}$ products are noticeably higher than those of Rh−C_{aryl} and Rh−C_{alkyl} analogues. The relationship between M−C and C−H bond strengths showed a linear correlation (slope $R_{M-C/H-C}$ = 1.32), and follows energy correlations previously established for unsubstituted sp^2 and sp^3 C−H bonds in aliphatic and aromatic hydrocarbons.

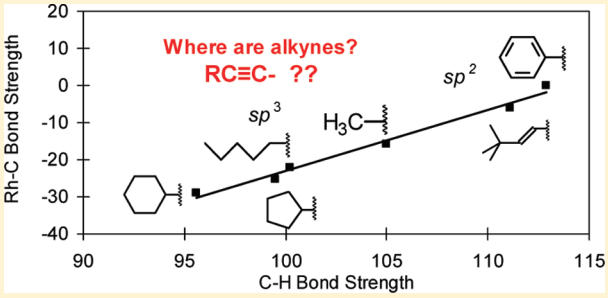

INTRODUCTION

Direct C−H bond activation and functionalization of hydrocarbons by homogeneous transition metal compounds has attracted interest due to its potential for industrial and synthetic applications. Issues of current interest center around conversion of C−H activated species to functionalized products and control of selectivity during the activation process.[1] For example, while ortho-directing groups have been widely employed for arene functionalization,[2] recent reports show that directed meta-[3] and para-[4] functionalization can also be obtained.

One important aspect of selectivity in organometallic C−H bond activation relies upon knowledge of metal−carbon bond strengths. While some examples of C−H activation take advantage of kinetic selectivity, many examples show that thermodynamic activation products are ultimately obtained.[5,6] Consequently, the importance of knowing relative metal−carbon bond strengths plays a critical role in predicting chemical reactivity. While many organometallic complexes have been shown to activate C−H bonds, only a few studies of kinetic and thermodynamic selectivity have been reported where bond strength information has been obtained.

In one early report, Marks et al. used calorimetry to determine a small series of zirconium−carbon and thorium−carbon bond strengths, noting a linear correlation versus C−H bond strengths in which D_{M-C} plotted against D_{C-H} displayed slopes, denoted herein by $R_{M-C/H-C}$, of 1.55 and 1.11, respectively.[7] Wolczanski et al. used exchange reactions to determine relative titanium−carbon bond strengths for over a dozen hydrocarbons, showing a relation between D_{M-C} and D_{C-H} with $R_{M-C/H-C}$ = 1.36.[8] Wolczanski also reported a more limited study of tantalum−carbon bond strengths in which the $R_{M-C/H-C}$ relating differences in M−C versus C−H bond strengths was 1.0.[9]

Early studies in our group established that in Cp*Rh(PMe_3)(R)H complexes, the range of metal−carbon bond strengths exceeded the range of C−H bond strengths, resulting in a thermodynamic preference for cleaving the stronger C−H bond due to the formation of an even stronger Rh−C bond.[10] Our group has also reported that generation of the [Tp′Rh(CNneopentyl)] (Tp′ = hydridotris-(3,5-dimethylpyrazolyl)-borate) fragment by photolysis of Tp′Rh(CNneopentyl)(η^2-PhN=C=N-neopentyl), **1**, in hydrocarbons leads to the clean activation of a C−H bond, giving Tp′Rh(CNneopentyl)(R)H (R = vinyl, alkyl, and aromatic). By combining kinetic barriers to reductive elimination with kinetic competition experiments, the thermodynamics for hydrocarbon exchange could be determined versus benzene ($\Delta G°$, Figure 1, eq 1). $\Delta G°$ was then used to determine relative rhodium−carbon bond strengths for 8 different hydrocarbon C−H bonds with sp^2 and sp^3 hybridization, showing a bond strength correlation with $R_{M-C/H-C}$ = 1.22.[11,12]

$$\Delta G° = \Delta G_{re}^{\ddagger}[Rh](Ph)H + \Delta\Delta G_{oa}^{\ddagger} - \Delta G_{re}^{\ddagger}[Rh](R)H \quad (1)$$

Received: February 2, 2012
Published: May 23, 2012

   dx.doi.org/10.1021/ja301095r | *J. Am. Chem. Soc.* 2012, 134, 9276−9284

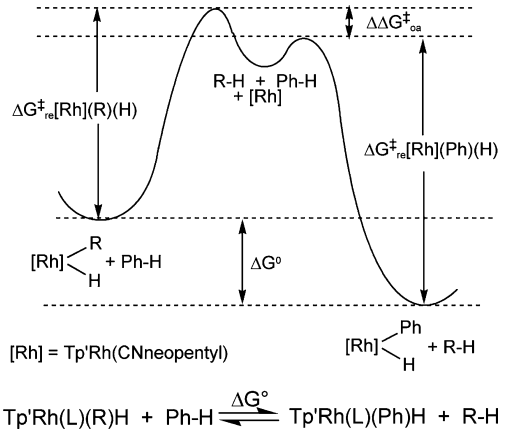

Figure 1. Free energy diagram for activation of hydrocarbon C−H bonds with [Tp′Rh(CNneopentyl)].

Perutz and Eisenstein reported DFT calculated results comparing Re-aryl^F and C−H bond strengths in the complex $CpRe(CO)_2(Ar^F)H$ for a complete series of polyfluorobenzenes, resulting in a bond strength correlation with $R_{M-C/H-C}$ = 2.25.[13] They calculated a similar effect on metal−aryl^F bond energies for a range of metal fragments, including $ZrCp_2$, $TaCp_2H$, $TaCp_2Cl$, WCp_2, $ReCp(CO)_2$, $ReCp(CO)(PH_3)$, $ReCp(PH_3)_2$, $RhCp(PH_3)$, $RhCp(CO)$, $IrCp(PH_3)$, $IrCp(CO)$, $Ni(H_2PCH_2CH_2PH_2)$, and $Pt(H_2PCH_2CH_2PH_2)$. In this series, $R_{M-C/H-C}$ values ranging from 1.93 to 3.05 were calculated.[14] More recently, our group studied C−H activation in a series of polyfluorobenzenes using both [Tp′Rh(CNneopentyl)] and [Tp′Rh(PMe_2Ph)] fragments.[15,16] In both of these experimental studies, kinetic measurements were used to correlate M−aryl^F bond strengths with aryl^F−H bond strengths, giving $R_{M-C/H-C}$ values of 2.14 and 2.15, respectively, showing that phosphine versus isocyanide spectator ligand had little effect on the range of metal−carbon bond strengths encountered.

Eisenstein and Perutz also performed DFT calculations of metal−carbon bond strengths with varioius hydrocarbons for both the Tp′Rh(CNneopentyl)(R)(H) and Ti(R)(silox)$_2$(NHSi^{t}Bu$_3$) (silox = OSi^{t}Bu$_3$) systems described above. Excellent agreement with experiment was seen for the calculated slopes of M−C versus C−H bond strengths ($R_{M-C/H-C}$ = 1.23 and 1.12, respectively).[17]

In all of the above studies, activations were limited to hydrocarbons containing sp^2 and sp^3 C−H bonds. Correlations with sp C−H bond activations are notably absent. Therefore, new studies aimed at further developing knowledge of C−H bond strengths of terminal alkynyl complexes of the [Tp′Rh(CNneopentyl)] fragment have been conducted and provide additional insight. Here, we report the use of reductive elimination rates and kinetic selectivity experiments to measure the relative free energy for the reaction of [Tp′Rh(CNneopentyl)] with various terminal alkynes (eq 2). The free energy will be used in concert with calculated bond strengths for terminal alkyne C−H bonds to ultimately determine relative M−C bond strengths for complexes of the type [Tp′Rh(CNneopentyl)(C≡CR)H]. A plot of ΔD(M−C) versus D(C−H) will be compared to computational results, and the factors that influence metal−carbon bond energies will be analyzed and quantified.

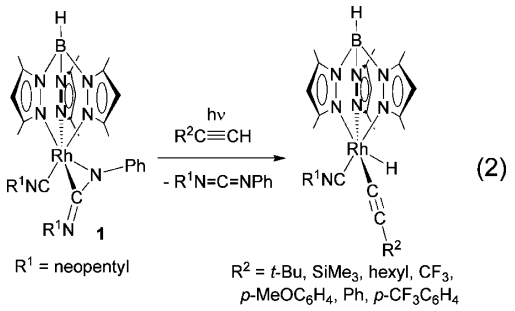

RESULTS AND DISCUSSION

C−H Bond Activation of Terminal Alkynes. The ability of Tp′Rh(CNneopentyl)(PhNCNneopentyl) (**1**) to serve as a photoprecursor to the reactive [Tp′Rh(CNR)] fragment has been well-established.[18] Irradiation of **1** in neat 3,3-dimethyl-1-butyne results in the loss of the carbodiimide ligand and insertion into the terminal C−H bond of the alkyne, producing a bright red solution. Removal of the solvent followed by ^{1}H NMR analysis of the residue in benzene-d_6 shows the clean formation of Tp′Rh(CNneopentyl)(C≡C−t-Bu)H (**2a**), which features a hydride doublet at δ −13.68 (J_{Rh-H} = 18.9 Hz, Scheme 1). An analogous photolysis of **1** in ethynyltrimethylsilane at 0 °C results in the formation of two hydride-containing products in a 1:1 ratio. The ^{1}H NMR spectrum displays two hydride resonances at δ −13.44 (d, J_{Rh-H} = 19.0 Hz) and −14.85 (d, J_{Rh-H} = 21.3 Hz), indicating the formation of both Tp′Rh(CNneopentyl)(C≡CSiMe$_3$)H (**3a**) and Tp′Rh(CNneopentyl)(CH$_2$SiMe$_2$C≡CH)H (**3b**). Complex **3b** is unstable in benzene solution at room temperature and the

Scheme 1. Products of Photolysis of 1 in Various Terminal Alkynes

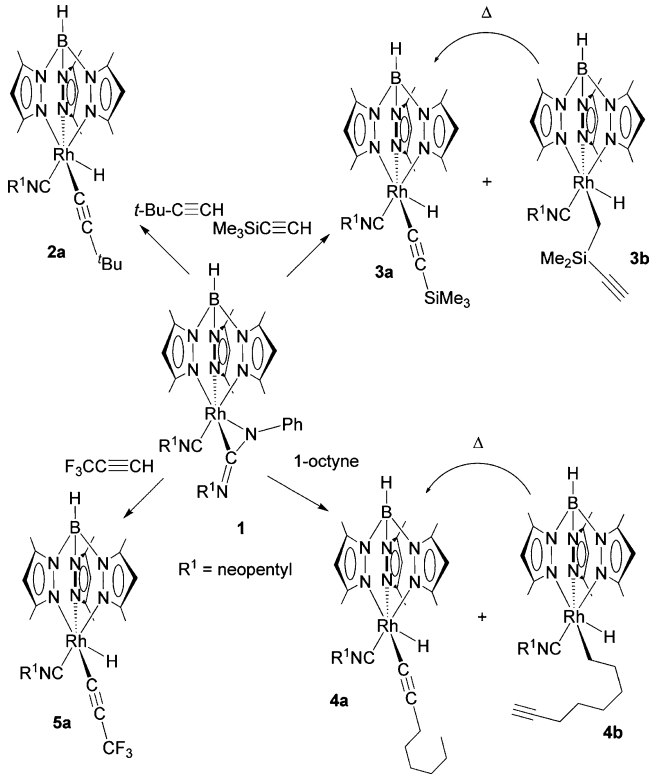

dx.doi.org/10.1021/ja301095r | J. Am. Chem. Soc. 2012, 134, 9276−9284

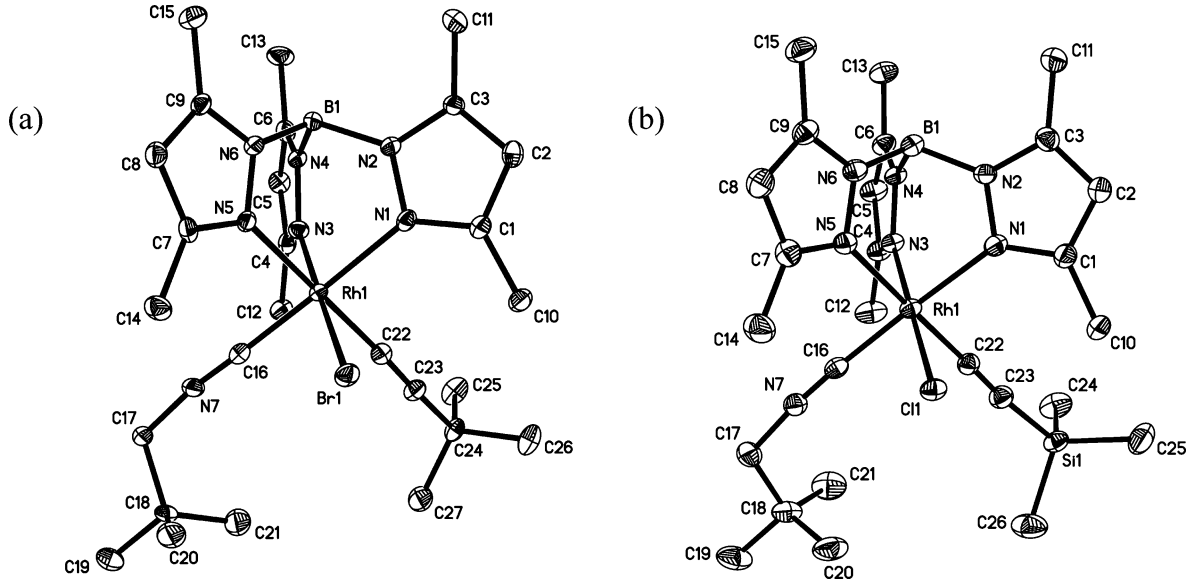

Figure 2. ORTEP drawing of the molecular structures of (a) **2a-Br** and (b) **3a-Cl**. All hydrogen atoms are omitted for clarity. Ellipsoids are shown at the 50% probability level.

hydride resonance at δ −14.85 disappeared in 2 days. The most notable resonances in the ^{1}H NMR spectrum of **2a** and **3a** are those for the hydrides which appear as doublets at δ −13.68 (d, J_{Rh-H} = 18.9 Hz) and −13.44 (d, J_{Rh-H} = 19.0 Hz), with a small J_{Rh-H} that is characteristic of an adjacent alkynyl ligand (vide infra). The complexes are chiral at rhodium, resulting in six resonances between δ 1.47 and 2.90 for the six Tp′ methyl groups and three resonances between δ 5.57 and 5.82 for the three Tp′ methyne hydrogens.

2a and **3a** can be halogenated with $CHBr_3$ or CCl_4, resulting in the formation of Tp′Rh(CNneopentyl)(C≡C−*t*-Bu)Br (**2a-Br**) or Tp′Rh(CNneopentyl)(C≡CSiMe$_3$)Cl (**3a-Cl**). Typical spectroscopic features are the low-field signals for the acetylide carbon atoms of Rh−C≡C unit in the ^{13}C{^{1}H} NMR spectra at δ 67.34 (J_{Rh-C} = 40.5 Hz, α-C) and 108.70 (J_{Rh-C} = 6.2 Hz, β-C) for **2a-Br** and δ 108.1 (J_{Rh-C} = 5.7 Hz, β-C) and 109.1 (J_{Rh-C} = 38.5 Hz, α-C) for **3a-Cl**, both of which are split into doublets. The IR spectra of **2a-Br** and **3a-Cl** display bands at 2158 and 2115 cm^{-1}, respectively, being assigned to the ν(C≡C) stretching modes of the alkynyl ligand.

The molecular structures of the rhodium complexes **2a-Br** and **3a-Cl** were determined by X-ray crystallographic analysis (Figure 2), and selected bond distances and angles are listed in Table 1. The coordination environments around the rhodium center of **2a-Br** and **3a-Cl** are essentially the same, and each rhodium atom possesses the κ^3-coordinated Tp′ ligand. The distances C(22)−C(23) for **2a-Br** and **3a-Cl** are 1.201(8) and 1.206(3) Å, respectively, indicating the presence of a C−C triple bond. The Rh−C(sp) distances are 1.975(6) and 1.970(2) Å, respectively, and are noticeably shorter than the Rh−C(sp^2) distance in Tp′Rh(CNneopentyl)(C$_6$F$_5$)Cl (2.063(5) Å)[19] and Tp′Rh(CNneopentyl)(CH=CHCMe$_3$)Cl (2.021(6) Å).[12]

Photolysis of **1** in 1-octyne gives two major hydride-containing products in a 1.2:1 ratio with trace amount of two more minor hydride-containing products, along with the commonly observed trace amounts of *o*-, *m*-, and *p*-carbodiimide activation products. Because of the number of products formed in this reaction, it was not possible to fully characterize each species individually by ^{1}H NMR spectroscopy. The two major hydride resonances at δ −13.66 (J_{Rh-H} = 19.2 Hz) and −14.91 (J_{Rh-H} = 24.6 Hz) are assigned as Tp′Rh(CNneopentyl)(C≡C-hexyl)H (**4a**) by comparison of Rh−H coupling with previous terminal alkyne activation products and Tp′Rh(CNneopentyl)[(CH$_2$)$_6$(C≡CH)]H (**4b**) by analogy to the previous report of Tp′Rh(CNneopentyl)(pentyl)(H).[11]

Table 1. Selected Bond Distances (Å) and Angles (deg) of 2a-Br and 3a-Cl

	2-Br		
Rh−Br	2.4671(10)	Rh−C16	1.911(6)
Rh−N1	2.090(5)	C22−C23	1.201(8)
N7−C16	1.147(7)	C22−Rh−N1	91.8(2)
		N1−Rh−Br	91.90(12)
C16−Rh−N1	177.2(2)	Rh−C22−C23	176.9(5)
Rh−C22	1.975(6)	C22−C23−C24	179.9(6)
	3a-Cl		
Rh−Cl	2.3566(5)	Rh−C16	1.932(2)
Rh−N1	2.0872(17)	C22−C23	1.206(3)
N7−C16	1.143(3)	C22−Rh−N1	91.87(7)
		N1−Rh−Cl	91.33(5)
C16−Rh−N1	178.03(7)	Rh−C22−C23	178.8(2)
Rh−C22	1.9703(19)	C22−C23−Si1	173.6(2)

Photolysis of **1** in pentane followed by pressurization with 3,3,3-trifluoro-1-propyne (10 psi) for 2 days at room temperature gives one hydride-containing product along with carbodiimide activation products (eq 3). Loss of pentane occurs

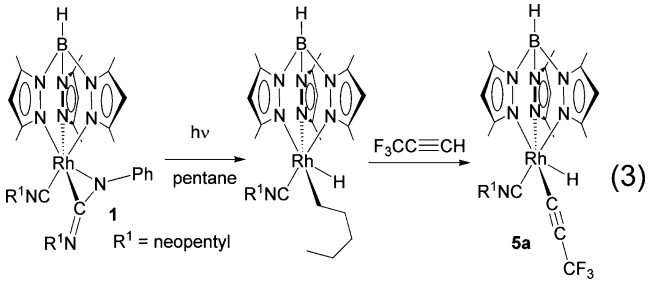

(3)

dx.doi.org/10.1021/ja301095r | J. Am. Chem. Soc. 2012, 134, 9276−9284

readily under these conditions ($\tau_{1/2} \approx 1$ h), and oxidative addition of 3,3,3-trifluoro-1-propyne proceeds to give **5a**. Removal of the solvent under vacuum followed by dissolving the residue in C_6D_6 allows observation of the hydride resonance for **5a** at δ −13.18 (d, J_{Rh-H} = 18.0 Hz). However, the reaction showed low conversion to **5a** and predominantly went to decomposition products. Consequently, Tp′Rh(CNneopentyl)(C≡CCF$_3$)H (**5a**) could not be fully characterized by ^{1}H NMR spectroscopy.

Photolysis of **1** in 4-ethynylanisole, phenylacetylene, and 4-ethynyl-α,α,α-trifluorotoluene showed 3 major products resulting from *o*-, *m*-, and *p*-carbodiimide activation at δ −13.39, −13.66, and −13.68 (Figure 3). Each spectrum shows

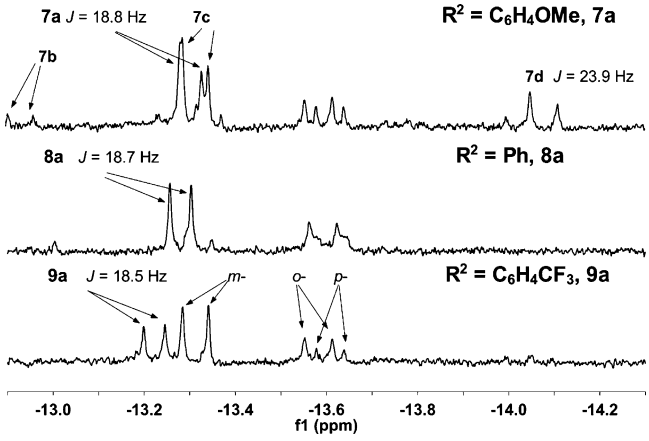

Figure 3. Hydride resonances for photolysis of **1** with 4-ethynylanisole, phenylacetylene, and 4-ethynyl-α,α,α-trifluorotoluene in the ^{1}H NMR spectrum. *o*-, *m*-, and *p*- mark the presence of carbodiimide activation side-products.

a terminal C−H bond activation product (**7a**, **8a**, **9a**), which has a J_{Rh-H} coupling constant of ∼19 Hz. There is also evidence for other products resulting from activation of the arene C−H bonds (**7b**, **7c**, **8b**, **8c**, **8d**, **9b**, **9c**), as these doublets have larger couplings (∼24 Hz), but overlap with each other and cannot be clearly identified. Methoxy group activation product **7d** (J_{Rh-H} = 23.9 Hz) was also observed in the reaction with 4-ethynylanisole.

To exclude carbodiimide activation products for a more precise observation of the Rh−H resonances in the ^{1}H NMR spectra, Tp′Rh(CNneopentyl)(CH$_3$)H (**6**) was prepared by the reaction of Tp′Rh(CNneopentyl)(CH$_3$)Cl with Cp$_2$ZrHCl/Cp$_2$ZrH$_2$ in THF followed by flash chromatography through silica gel to give Zr-free solutions of **6**.[20] Addition of 4-ethynylanisole, phenylacetylene, or 4-ethynyl-α,α,α-trifluorotoluene to **6** in benzene at room temperature gave the terminal C−H bond activation products **7a**, **8a**, or **9a**, along with aryl ring activation products **7b**−**9c** (eq 4) and some phenyl hydride Tp′Rh(CNneopentyl)(Ph)H, **10**. The reaction with 4-ethynylanisole shows four hydride resonances at δ −13.37 (J_{Rh-H} = 18.8 Hz) for the alkyne C−H activation product **7a**, −14.18 (J_{Rh-H} = 24.1 Hz) for the methoxy group activation product **7d**, and −13.03 (J_{Rh-H} = 22.8 Hz) and −13.44 (J_{Rh-H} = 21.6 Hz) for the phenyl ring activation products **7b** and **7c**. The reaction with phenylacetylene also showed four hydride resonances at δ −13.34 (J_{Rh-H} = 18.7 Hz) for the terminal alkyne C−H activation product **8a** and at δ −13.05 (J_{Rh-H} = 23.4 Hz), −13.33 (J_{Rh-H} = 23.6 Hz), and −13.68 (J_{Rh-H} = 22.1 Hz) for phenyl ring activation products **8b**−**d**. However, the

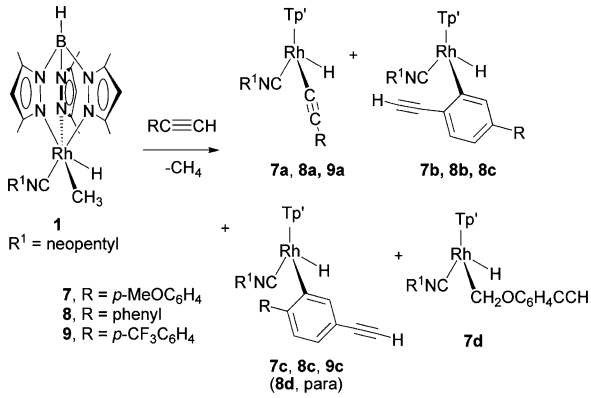

(4)

reaction with 4-ethynyl-α,α,α-trifluorotoluene showed only one hydride resonance at δ −13.29 (J_{Rh-H} = 18.5 Hz) for the terminal alkyne C−H activation product **9a** (Figure 4).

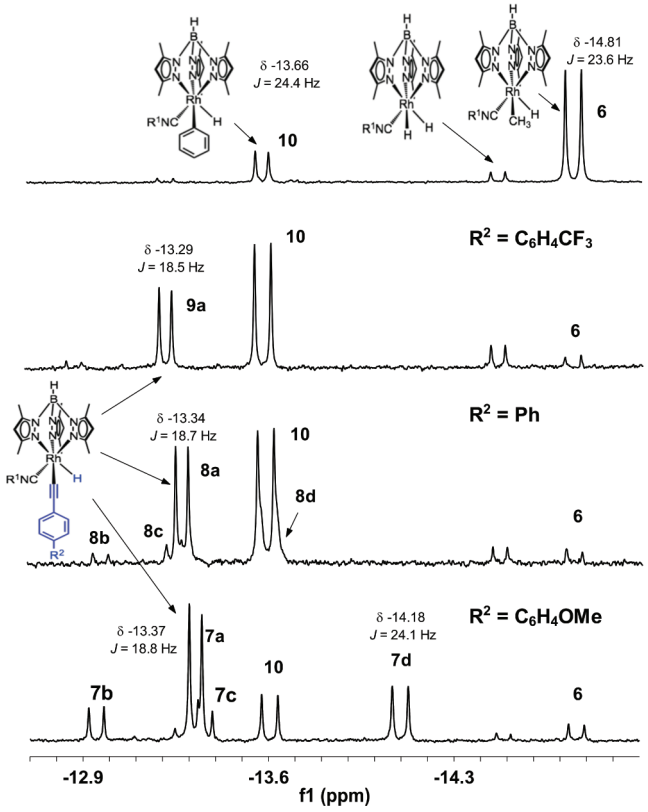

Figure 4. ^{1}H NMR hydride resonances of 4-ethynylanisole, phenylacetylene, and 4-ethynyl-α,α,α-trifluorotoluene activation complexes formed by reductive elimination of methane from **6**. Note that some Tp′Rh(CNneopentyl)H$_2$ is seen from the preparation of Tp′Rh(CNneopentyl)(Me)H using Cp$_2$ZrH$_2$ (top spectrum).

As the above routes to the arylalkynyl complexes were not very selective, these complexes were synthesized independently. The alkynyl rhodium complexes, **7a-Cl**, **8a-Cl**, and **9a-Cl** were prepared by treatment of Tp′Rh(CNneopentyl)Cl$_2$ with magnesium acetylides in order to exclude the aryl hydride products seen in the C−H activation reactions (see Supporting Information, for the molecular structure of **8-Cl**). Each alkynyl rhodium chloride complex reacted with LiEt$_3$BH to exchange chloride for hydride and gave clean formation of complexes **7a**,

dx.doi.org/10.1021/ja301095r | J. Am. Chem. Soc. 2012, 134, 9276−9284

8a, and **9a**, with hydride resonances identical to those shown in Figure 4 (eq 5).

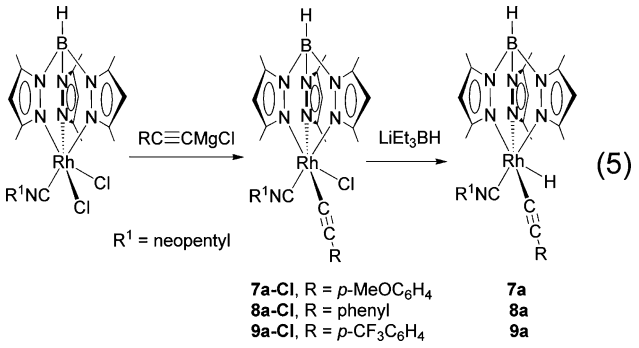

(5)

Reductive Elimination of RC≡CH from Tp′Rh(CNR)(C≡CR)(H). The rates of reductive elimination of alkyne from complexes **2a**, **3a**, **4a**, **5a**, and **7a**–**9a** were determined in C_6D_6 solution by monitoring the conversion of the complexes to Tp′Rh(CNneopentyl)(C_6D_5)D (**10**-d_6) by ^{1}H NMR spectroscopy (eq 6). These experiments were performed at 100 °C, and

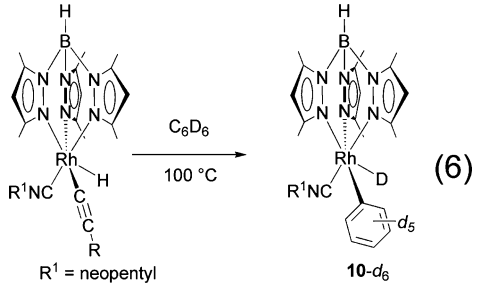

(6)

in each case, formation of **10**-d_6 was irreversible. Pentafluorobenzene was used instead of benzene to trap the [Tp′Rh(CNneopentyl)] fragment in cases where decomposition occurs prior to the formation of **10**-d_6 due to the extended reaction times and elevated temperatures. A plot of ln($[C]_t/[C]_0$) of the terminal C–H bond activation complex versus time was used to determine the rates of reductive elimination. Table 2 summarizes the rate constants k_{re}(RC≡CH) along with the activation energies for the reductive elimination at 100 °C ($\Delta G^{\ddagger}_{re}$).

The rate of reductive elimination of terminal alkynes is slow compared to alkane or benzene reductive elimination. Complete conversion to **10**-d_6 in C_6D_6 was observed for complexes **2a**–**5a**, while complexes **7a**–**9a** led to decomposition. It is possible that η^2-coordination of phenylacetylene derivatives stabilizes the [Tp′Rh(CNneopentyl)] fragment and inhibits the formation of the benzene activation product when its reductive coupling is achieved, although these adducts were not observed. When pentafluorobenzene was used to trap the metal fragment, however, the perfluorophenyl hydride product is observed, but not quantitatively (30–60%). Consequently, these barriers for reductive elimination should be considered as a lower limit for the barrier for dissociative reductive elimination. One can observe the slowing of the rate of reductive elimination as one changes phenyl substitution to an electron-withdrawing group (CF_3) in the para position of the phenyl ring of phenylacetylene.

Table 2. Rates of Reductive Elimination of RC≡CH from Tp′Rh(CNneopentyl)(C≡CR)(H) at 100 °C[a]

R	k_{re}(RC≡CH), s^{-1}	$\Delta G^{\ddagger}_{re}$, kcal mol^{-1}
3,3-dimethyl-1-butyne	6.7 (3) × 10^{-6}	30.83 (4)
ethynyltrimethylsilane	7.1 (6) × 10^{-7}	32.50 (6)
1-octyne	1.21 (7) × 10^{-5}	30.39 (4)
3,3,3-trifluoro-1-propyne	1.8 (2) × 10^{-5}	30.10 (8)
4-ethynylanisole	7.2 (4) × 10^{-6}	30.78 (4)
phenylacetylene	2.6 (1) × 10^{-6}	31.53 (4)
4-ethynyl-α,α,α-trifluorotoluene	1.7 (1) × 10^{-6}	31.83 (5)

[a]Errors are reported as standard deviations. Error in $\Delta G^{\ddagger}_{re}$ calculated using $\sigma_G = -(RT/k_{re})\sigma_k$.

Competition Experiments. The rate at which two substrates compete for the vacant site in [Tp′Rh(CNneopentyl)] was determined by irradiation of **1** in a known ratio of two substrates and monitoring the kinetic products formed by ^{1}H NMR spectroscopy (Table 3). In competition experiments where multiple sites were activated, only the quantity of terminal alkyne activation product was used in calculating the k_1/k_2 product ratio. Consequently, the quantity of methyl activation product of ethynyltrimethylsilane and *o*-, *m*-, and *p*-phenyl ring activation products of phenylacetylene derivatives were not used in the competition experiment calculations, as these represent side-reactions. The selectivities $k_{substrate}/k_{C6H6}$ reported in Table 3 were calculated on a per-molecule basis using eq 7, where I_1/I_2 is the integrated area of the hydrides of the products, V_2/V_1 is the ratio of the substrate volumes, d_2/d_1 is the solvent density ratio, and MW_1/MW_2 is the ratio of molecular weights; subscript 2 refers to benzene/pentane/mesitylene and subscript 1 refers to the competing terminal alkyne. For the competitions of alkynes versus pentane and mesitylene, these ratios were converted to be relative to benzene as indicated in Table 3 using competition data from ref 11. The mild selectivities resulted in small differences in $\Delta\Delta G^{\ddagger}_{oa}$ values (<1.2 kcal mol^{-1}).

Table 3. Kinetic Selectivity Data Determined from Competition Experiments[a]

entry	substrates	T (°C)	$k_{substrate}/k_{C6H6}$	$\Delta\Delta G^{\ddagger}_{oa}$, kcal mol^{-1}[b]
1	3,3-dimethyl-1-butyne: benzene	10	0.18 (3)	1.0 (1)
2	ethynyltrimethylsilane: benzene	10	0.33 (5)	0.6 (1)
3	1-octyne: mesitylene[c]	10	0.12 (2)[c]	1.2 (1)
4	3,3,3-trifluoro-1-propyne: pentane[d]	10	0.26 (4)[d]	0.8 (1)
5	4-ethynylanisole: benzene	10	0.60 (9)	0.3 (1)
6	phenylacetylene: benzene	10	0.41 (6)	0.5 (1)
7	4-ethynyl-α,α,α-trifluorotoluene: benzene	10	1.2 (2)	−0.1 (1)

[a]All samples were irradiated for 10 min using same equivalent volume ratio of each substrate used. Ratios are then corrected to be relative to benzene, if necessary. No correction for the number of hydrogens available has been applied. [b]$\Delta\Delta G^{\ddagger}$ vs benzene. A negative value indicates that terminal alkyne is kinetically favored. Errors in rate ratio estimated at 15%, giving $\sigma_G = -(RT/\text{ratio})\sigma_{ratio} = -0.15RT \approx 0.1$ kcal mol^{-1}. [c]$k_{octyne}/k_{benzene} = (k_{octyne}/k_{mesitylene})(k_{mesitylene})/k_{benzene}) = (0.154)(0.769) = 0.118$. [d]$k_{CF3C\equiv CH}/k_{benzene} = (k_{CF3C\equiv CH}/k_{pentane})(k_{pentane})/k_{benzene}) = (1.22)(0.213) = 0.259$.

$$\frac{k_{substrate}}{k_{C6H6}} = \left(\frac{I_1}{I_2}\right)\left(\frac{V_2}{V_1}\right)\left(\frac{d_2}{d_1}\right)\left(\frac{MW_1}{MW_2}\right) \quad (7)$$

dx.doi.org/10.1021/ja301095r | J. Am. Chem. Soc. 2012, 134, 9276–9284

Table 4. Kinetic and Thermodynamic Data for Formation of Tp′Rh(CNneopentyl)(R)H[a]

R (terminal C−H)	$\Delta\Delta G^{\ddagger}_{oa}$ [b]	ΔG° [b]	calcd D(C−H)[c]	exptl D_{rel}(Rh−C)[d]	calcd D_{rel}(Rh−C)[d,e]
3,3-dimethyl-1-butyne	1.0 (1)	1.1 (2)	131.4	18.4	26.9
ethynyltrimethylsilane	0.6 (1)	−0.9 (2)	131.6	20.6	27.1
1-octyne	1.2 (1)	1.8 (2)	131.0	17.4	26.4
3,3,3-trifluoro-1-propyne	0.8 (1)	1.7 (2)	135.4	21.9	37.4
4-ethynylanisole	0.3 (1)	−0.5 (2)	122.7	10.4	24.2
phenylacetylene	0.5 (1)	−0.0 (2)	133.2	21.4	27.6
4-ethynyl-α,α,α-trifluorotoluene	−0.1 (1)	−0.9 (2)	127.8	16.9	31.9

[a]All values are in kcal mol^{-1}. Cumulative errors in all D's are estimated at 0.3 kcal mol^{-1} plus any uncertainty in the D_{C-H} (calculated D_{C-H} do not have errors). [b]$\Delta\Delta G^{\ddagger}_{oa}$ and ΔG° vs benzene. A positive value means benzene is favored. [c]Calculated using DFT; B3LYP/6-31 g**. [d]Relative to D(Rh−Ph) = 69.4 kcal mol^{-1}. A positive value means $D_{Rh-C\equiv CR}$ is stronger. [e]Calculated using DFT; M06-2X/6-31g**.

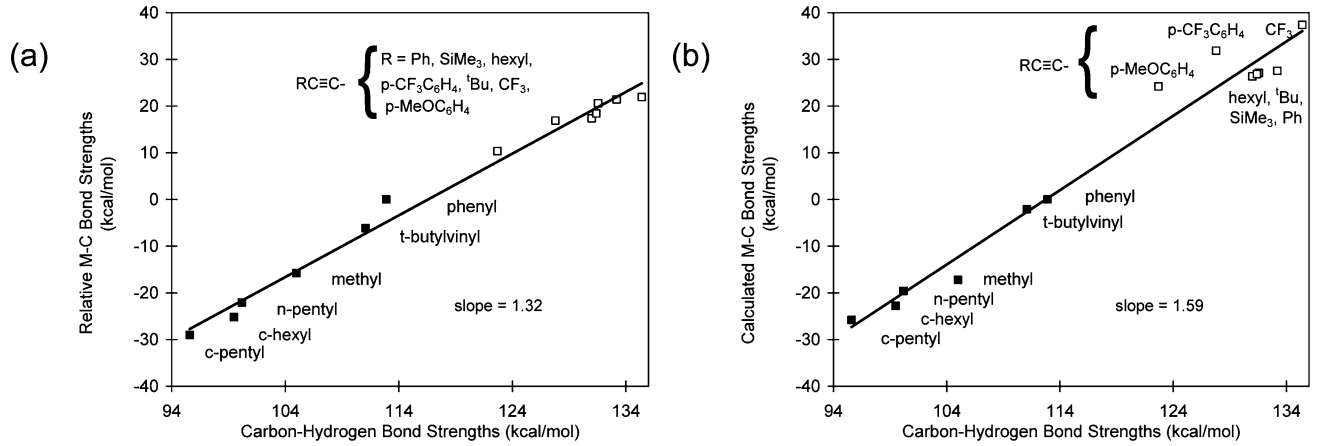

Figure 5. Plot of relative Rh−$C_{alkynyl}$ bond strength vs terminal C−H bond strength of terminal alkynes (kcal mol^{-1}). (a) Experimentally determined D(Rh−$C_{alkynyl}$) vs experimental (■)/DFT-calculated (□) D(C−H), and (b) DFT-calculated D(Rh−$C_{alkynyl}$) vs experimental (■)/DFT-calculated (□) D(C−H).

Analysis of Rhodium−Carbon Bond Strengths. From these kinetic selectivities ($\Delta\Delta G^{\ddagger}$) and reductive elimination barriers ($\Delta G^{\ddagger}_{re}$), the driving force ΔG° relative to benzene activation can be calculated as indicated in eq 1. One feature of this method is that the uncertanties in G are small, since free energy (G) is a log function of rate (k) or rate ratio (k_1/k_2). Next, the relative metal−carbon bond strengths can be calculated as indicated in eq 8. Here, the driving force (free energy) is related to the differences in metal−carbon and carbon−hydrogen bond strengths (enthalpy), along with an entropic correction for the number of hydrogens available for activation (1 vs 6). Since only the C−H bond strength for phenylacetylene is reported in the literature,[21] the C−H bond strengths shown in Table 4 were calculated using DFT.

$$\begin{aligned} D_{rel}(\text{Rh−C}) &= [\Delta H(\text{Rh−CCR}) - \Delta H(\text{Rh−Ph})] \\ &= \Delta G^{\circ} - RT\ln(1/6) \\ &\quad - [D(\text{RCC−H}) - D(\text{Ph−H})] \end{aligned} \tag{8}$$

These data are also shown graphically in Figure 5a, in which the relative metal−carbon bond strength is plotted versus the carbon−hydrogen bond strength. Included in the plot are data from earlier studies with sp^3 and sp^2 hydrocarbons, but not substrates in which the C−H bond is effected by resonance (e.g., H−CH_2CN, H−CH_2Ph, H−CH_2CH=CH_2).[22] Good linearity is observed for all of these 'normal' sp, sp^2, sp^3 hydrocarbons. A slope $R_{M-C/H-C}$ = 1.32 is observed, which indicates that the differences in metal−carbon bond energies are about 30% greater than the difference in carbon−hydrogen bond energies.

For comparison with the experimental values for this system, DFT calculations were performed on the corresponding terminal alkyne complexes using the model fragment [Tp′Rh(CNMe)] (see Supporting Information). These calculated Rh−$C_{alkynyl}$ bond strengths are also listed in Table 4, and calculated Rh−C bond strengths for the other hydrocarbons were reported earlier.[23] A plot of C−H bond strengths[21] versus *calculated* Rh−C bond strengths (M06-2X) in Tp′Rh(CNMe)(R)H shows dispersion of terminal alkynes with $R_{M-C/H-C}$ = 1.59 (Figure 5b). The DFT calculations appear to slightly overestimate the differences in rhodium−carbon bond strengths, but the magnitude of the slope depends on the method and model employed. We examined methods M06-2X, B3LYP, and B3PW91 and models TpRh(CNMe), Tp*Rh(CNMe), TpRh(CNC$H_2{}^t$Bu), and Tp*Rh(CNC$H_2{}^t$Bu), with M06-2X and Tp*Rh(CNMe) giving reasonable agreement with experiment (see Supporting Information for details).

In addition, DFT was used to calculate the effect of changing the R group attached to rhodium on the metal−hydrogen bond strength. For each of the complexes Tp′Rh(CNMe)(R)H, the Rh−H bond strength was calculated. The variation of Rh−H bond strengths was minimal (68.6 ± 1.2 kcal mol^{-1}), indicating that the differences in the stability of the various derivatives lies in changes of the Rh−C bond strength, not in changes of the Rh−H bond strength as a result of the change in alkynyl ligand (see Supporting Information for details).

It is also worth noting that terminal alkynes, with the strongest C−H bonds of all hydrocarbons, also have the

dx.doi.org/10.1021/ja301095r | J. Am. Chem. Soc. 2012, 134, 9276−9284

strongest metal−carbon bonds. This results in alkynes being the 'king' in thermodynamic competitions with all other hydrocarbons. In terms of kinetic selectivity with [Tp′Rh(CNneopentyl)], the range of competitive selectivities is small, spanning a range of only a factor of 22:1 for the very best substrate (4-ethynyl-α,α,α-trifluorotoluene) to the very worst substrate (cyclohexane). Finally, it is also worth noting that these reactions give clean terminal alkyne C−H activation products. No evidence for rearrangement to terminal vinylidene compounds has been seen, in contrast to the reactions with $RhCl(P^iPr_3)_3$[24] and numerous other transition metal complexes.[25]

CONCLUSIONS

Photolysis of Tp′Rh(CNneopentyl)(η^2-PhNCNneopentyl) in neat terminal alkynes resulted in C−H activation products of the type Tp′Rh(CNneopentyl)(C≡CR)H (R = *t*-Bu, $SiMe_3$, hexyl, CF_3, *p*-$OMeC_6H_4$, Ph, *p*-$CF_3C_6H_4$). The arylalkyne derivatives could be prepared pure via an acetylation/hydride exchange sequence. Measurement of the barriers to alkyne reductive elimination, along with kinetic selectivity for terminal C−H activation versus benzene, allowed for the determination of the driving force for a given C−H activation versus C−H activation of benzene. These data, in turn, allow the determination of relative metal−acetylide bond strengths. Plotting the experimentally determined $D(Rh-C_{alkynyl})$ versus calculated C−H bond strengths gives a slope $R_{M-C/H-C}$ of 1.32, and this work completes a connection of sp C−H activation to related rhodium−carbon bond energy correlations in unsubstituted sp^2 and sp^3 aliphatic and aromatic hydrocarbons. DFT calculated bond energies tend to exaggerate the differences in rhodium−carbon bond strengths, as the slope of this plot is 1.59.

EXPERIMENT SECTION

General Procedures. All operations and routine manipulations were performed under a nitrogen atmosphere, either on a high-vacuum line using modified Schelnk techniques or in a Vacuum Atmospheres Corp. Dri-Lab. Benzene-d_6 was distilled under vacuum from CaH_2 and stored in an ampule with a Teflon valve. Terminal alkynes were purchased from Aldrich Chemical Co. and TCI America, dried over CaH_2, and vacuum-distilled prior to use. Isopropyl-magnesium chloride was purchased from Aldrich. Preparations of Tp′Rh(CNneopentyl)(η^2−PhN=C=N−neopentyl) (**1**),[18] Tp′Rh(CNneopentyl)Cl_2,[26] and Tp′Rh(CNneopentyl)$(CH_3)H$[20] have been previously reported. All ^1H NMR, ^{19}F NMR, and ^{13}C NMR spectra were recorded on a Bruker Avance 400 and 500 MHz NMR spectrometer. IR spectra were recorded in the solid state on a Nicolet 4700 FTIR spectrometer between 4000 and 600 cm^{-1}. All photolysis experiments were carried out using a pyrex-filtered 200-W Hg−Xe lamp.

Computational Details. Homolytic C−H and Rh−C bond energies were calculated for the seven alkynes and TpRh(CNMe)(H)−C≡CR complexes, respectively, and are presented in Table 4. X-ray crystallographic structures were used as the starting points for the calculations if a corresponding structure was available. Gas-phase structures were fully optimized in redundant internal coordinates,[27] with density functional theory (DFT) and a wave function incorporating Becke's three-parameter hybrid functional (B3)[28] along with the Lee−Yang−Parr correlation functional (LYP).[29] The alkynyl complexes were also calculated using the M06-2X and B3PW91 functionals for comparison.[30] All calculations were performed using the Gaussian09 package.[31] The Rh and Si atoms were represented with the effective core pseudopotentials of the Stuttgart group and the associated basis sets improved with a set of f-polarization functions for Rh (alpha = 1.350)[32] and a set of d-polarization functions for Si (alpha = 0.284).[33] The remaining atoms (C, H, N, B, O, and F) were represented by a 6-31G(d,p)[34] basis set. The geometry optimizations were performed without any symmetry constraints, and the local minima were checked by frequency calculations. Gibbs free energies have been calculated at 298.15 K and 1 atm.

Preparation of Tp′Rh(CNneopentyl)(C≡CCMe$_3$)H (2a). A solution of **1** (10 mg, 0.017 mmol) dissolved in 0.6 mL of *t*-butylacetylene was placed in a J-Young NMR tube. This sample was irradiated for 5 min at 0 °C. The solvent was immediately removed in vacuo at room temperature. The resulting bright yellow residue was dissolved in C_6D_6. Only one C−H activation product was observed, consistent with the earlier observation that **1** does not activate neopentane.[11] ^1H NMR (400 MHz, C_6D_6): δ −13.68 (d, *J* = 18.9 Hz, 1 H, Rh-*H*), 1.13 (s, 9 H, $C(CH_3)_3$ of *t*-Bu-acetylene), 1.47 (s, 9 H, $C(CH_3)_3$), 2.11 (s, 3 H, pzCH_3), 2.18 (s, 3 H, pzCH_3), 2.26 (s, 3 H, pzCH_3), 2.30 (s, 3 H, pzCH_3), 2.53 (d, *J* = 4.5 Hz, 2 H, NCH_2), 2.75 (s, 3 H, pzCH_3), 2.90 (s, 3 H, pzCH_3), 5.57 (s, 1 H, pz*H*), 5.63 (s, 1 H, pz*H*), 5.82 (s, 1 H, pz*H*).

Preparation of Tp′Rh(CNneopentyl)(C≡CCMe$_3$)Cl (2a-Cl). A similar procedure to that for **7a-Cl** was employed. ^1H NMR (500 MHz, C_6D_6): δ0.88 (s, 9 H, $C(CH_3)_3$ of isocyanide), 1.45 (s, 9 H), 2.02 (s, 3 H), 2.11 (s, 3 H, pzCH_3), 2.15 (s, 3 H, pzCH_3), 2.68 (q, *J* = 13.6 Hz, 2 H, NCH_2), 2.76 (s, 3 H, pzCH_3), 2.78 (s, 3 H, pzCH_3), 3.26 (s, 3 H, pzCH_3), 5.55 (s, 1 H, pz*H*), 5.61 (s, 1 H, pz*H*) 5.63 (s, 1 H, pz*H*). ^{13}C NMR (500 MHz, C_6D_6): δ 12.28 (pzCH_3), 12.42 (pzCH_3), 12.68 (pzCH_3), 14.85 (pzCH_3), 15.83 (pzCH_3), 16.03 (pzCH_3), 26.76 ($C(CH_3)_3$ of isocyanide), 29.72 ($C(CH_3)_3$ of *t*-Bu-acetylene), 30.49 ($C(CH_3)_3$ of isocyanide), 30.49 ($C(CH_3)_3$ of *t*-Bu-acetylene), 56.24 (NCH_2), 67.34 (d, *J* = 40.5 Hz, Rh-CC-*t*-Bu), 107.34 (CH of pz), 107.68 (CH of pz), 108.13 (CH of pz), 108.70 (d, *J* = 6.2 Hz, Rh−CC-*t*-Bu), 142.72 (pzC_q), 143.08 (pzC_q), 144.22 (pzC_q), 151.99 (pzC_q), 152.16 (pzC_q), 154.42 (pzC_q). IR (cm^{-1}) ν = 1975, 2026, 2158 (C≡C). **2a-Cl** also forms upon treatment of **2a** with CCl_4.

Preparation of Tp′Rh(CNneopentyl)(C≡CCMe$_3$)Br (2a-Br). **2a-Br** was prepared by treatment of **2a** with $CHBr_3$, and crystals were grown for X-ray structure determination. ^1H NMR (500 MHz, C_6D_6): δ0.88 (s, 9 H, $C(CH_3)_3$ of isocyanide), 1.45 (s, 9 H), 2.02 (s, 3 H), 2.11 (s, 3 H, pzCH_3), 2.15 (s, 3 H, pzCH_3), 2.68 (q, *J* = 13.6 Hz, 2 H, NCH_2), 2.76 (s, 3 H, pzCH_3), 2.78 (s, 3 H, pzCH_3), 3.26 (s, 3 H, pzCH_3), 5.55 (s, 1 H, pz*H*), 5.61 (s, 1 H, pz*H*) 5.63 (s, 1 H, pz*H*). ^{13}C NMR (500 MHz, C_6D_6): δ 12.28 (pzCH_3), 12.42 (pzCH_3), 12.68 (pzCH_3), 14.85 (pzCH_3), 15.83 (pzCH_3), 16.03 (pzCH_3), 26.76 ($C(CH_3)_3$ of isocyanide), 29.72 ($C(CH_3)_3$ of *t*-Bu-acetylene), 30.49 ($C(CH_3)_3$ of isocyanide), 30.49 ($C(CH_3)_3$ of *t*-Bu-acetylene), 56.24 (NCH_2), 67.34 (d, *J* = 40.5 Hz, Rh-CC-*t*-Bu), 107.34 (CH of pz), 107.68 (CH of pz), 108.13 (CH of pz), 108.70 (d, *J* = 6.2 Hz, Rh−CC-*t*-Bu), 142.72 (pzC_q), 143.08 (pzC_q), 144.22 (pzC_q), 151.99 (pzC_q), 152.16 (pzC_q), 154.42 (pzC_q). IR (cm^{-1}) ν = 1975, 2026, 2158 (C≡C). Anal. Calcd for $C_{27}H_{42}BBrN_7Rh·1/2(THF)$: C, 50.16; H, 6.68; N, 14.12. Found: C, 49.56; H, 6.61; N, 13.18 (THF is observed in the X-ray structure).

Preparation of Tp′Rh(CNneopentyl)(C≡CSiMe$_3$)H (3a). The synthesis of **3a** was identical to that of **2a** except that **1** was dissolved in 0.6 mL of ethynyltrimethylsilane and the product solution was allowed to stand for 2 d at room temperature. At earlier times, Tp′Rh(CNneopentyl)(CH_2SiMe_2C≡CH)H (**3b**) could be observed. For **3a**, ^1H NMR (400 MHz, C_6D_6): δ −13.44 (d, *J* = 19.0 Hz, 1 H, Rh-*H*), 0.11 (s, 9 H, $Si(CH_3)_3$), 0.74 (s, 9 H, $C(CH_3)_3$), 2.11 (s, 3 H, pzCH_3), 2.16 (s, 3 H, pzCH_3), 2.26 (s, 3 H, pzCH_3), 2.27 (s, 3 H, pzCH_3), 2.76 (s, 3 H, pzCH_3), 2.86 (s, 2 H, NCH_2), 2.88 (s, 3 H, pzCH_3), 5.52 (s, 1 H, pz*H*), 5.61 (s, 1 H, pz*H*), 5.78 (s, 1 H, pz*H*). For **3b**, ^1H NMR (400 MHz, C_6D_6): δ −14.85 (d, *J* = 21.3 Hz, 1 H, Rh-*H*), 0.64 (s, 6 H, $Si(CH_3)_2$), 0.71 (s, 2 H, Rh−CH_2), 0.74 (s, 9 H, $C(CH_3)_3$), 2.05 (s, 3 H, pzCH_3), 2.17 (s, 3 H, pzCH_3), 2.29 (s, 3 H, pzCH_3), 2.40 (s, 3 H, pzCH_3), 2.47 (s, 3 H, pzCH_3), 2.60 (s, 5 H, 3 H of pzCH_3, 2 H of NCH_2), 5.59 (s, 1 H, pz*H*), 5.66 (s, 1 H, pz*H*), 5.82 (s, 1 H, pz*H*).

Preparation of Tp′Rh(CNneopentyl)(C≡CSiMe$_3$)Cl (3a-Cl). **3a-Cl** was obtained by treatment of **3a** with CCl_4. ^1H NMR (400

dx.doi.org/10.1021/ja301095r | J. Am. Chem. Soc. 2012, 134, 9276−9284

MHz, C_6D_6): δ 0.34 (s, 9 H, C(CH_3)$_3$), 0.87 (s, 9 H, Si(CH_3)$_3$), 2.02 (s, 3 H, pzCH_3), 2.10 (s, 3 H, pzCH_3), 2.14 (s, 3 H, pzCH_3), 2.68 (d, J = 5.7 Hz, 2 H), 2.73 (s, 3 H, pzCH_3), 2.76 (s, 3 H, pzCH_3), 3.23 (s, 3 H, pzCH_3), 5.52 (s, 1 H, pz$H$), 5.56 (s, 1 H, pz$H$), 5.63 (s, 1 H, pz$H$). $^{13}C\{^1H\}$ NMR (400 MHz, C_6D_6): δ 1.64 (Si(CH_3)$_3$), 12.26 (pzCH_3), 12.40 (pzCH_3), 12.68 (pzCH_3), 14.83 (pzCH_3), 15.9 (pzCH_3), 16.07 (pzCH_3), 26.72 (C(CH_3)$_3$), 32.55 (C(CH_3)$_3$), 56.28 (s, NCH_2), 107.41 (CH of pz), 107.83 (CH of pz), 108.1 (d, J = 5.7 Hz, Rh−$CCSiMe_3$),108.26 (CH of pz), 109.10 (d, J = 38.5 Hz, Rh-$CCSiMe_3$), 142.85 (pzC_q), 143.24 (pzC_q), 144.34 (pzC_q), 152.06 (pzC_q), 152.24 (pzC_q), 154.53 (pzC_q). IR (cm^{-1}) ν = 2088, 2115 (C≡C), 2325. Anal. Calcd for $C_{26}H_{42}BClN_7RhSi\cdot(C_6H_6)$: C, 54.28; H, 6.83; N, 13.85. Found: C, 53.85; H, 7.12; N, 13.25 (C_6H_6 is observed in the X-ray structure).

Preparation of Tp′Rh(CNneopentyl)(C≡C(CH_2)$_5$$Me_3$)H (4a). The synthesis of **4a** was identical to that of **2** except that **1** was dissolved in 0.6 mL of 1-octyne. Following photolysis, hydride resonances for both **4a** (δ −13.66, d, J = 19.2 Hz) and **4b** (δ −14.91, d, J = 24.6 Hz) were observed. After several hours at room temperature, only **4a** was observed.

Preparation of Tp′Rh(CNneopentyl)(C≡CCF_3)H (5a). Complex **1** was placed in a J-Young NMR tube, dissolved in pentane, and irradiated for 20 min at 10 °C, followed by pressurization with 3,3,3-trifluoro-1-propyne (10 psi). The mixture was kept for 2 days at room temperature and the solvent was removed under vacuum, yielding **5a**. For **5a**, ^1H NMR (400 MHz, C_6D_6): δ −13.18, d, J = 18.0 Hz.

Reaction of Tp′Rh(CNneopentyl)(CH_3)H with Arylalkynes. A solution of Tp′Rh(CNneopentyl)-(CH_3)H (**6**) in benzene solvent was prepared, the solvent removed and replaced with C_6D_6, and excess phenylacetylene added. The solution was monitored by ^1H NMR spectroscopy to determine the products formed as methane was eliminated. The observations of the hydride region of the spectrum are described in the text. Similar reactions were carried out with 4-ethynylanisole and 4-ethynyl-α,α,α-trifluorotoluene.

Preparation of Magnesium Acetylides. Isopropylmagnesium-chloride (0.17 mL of a 2 M solution in THF, 0.34 mmol) was added dropwise by syringe to phenylacetylene (38 μL, 0.34 mmol) in 3 mL of THF under an atmosphere of N_2. The reaction mixture was stirred for 1 h at room temperature following which the magnesium reagent was ready for use. The p-CF_3- and p-MeO-phenylethynyl reagents were prepared similarly.

Preparation of Tp′Rh(CNneopentyl)(C≡CC_6H_4-p-OMe)Cl (7a-Cl). To a stirred solution of 200 mg (0.35 mmol) of Tp′Rh(CNneopentyl)Cl_2 in 250 mL f THF was added, dropwise over a period of 2 min, a solution of the magnesium acetylide prepared as described above. Upon addition of the Grignard reagent, the color of the solution changed from yellow to green-yellow. The reaction mixture was stirred for 1 h. The reaction was quenched with a saturated solution of NH_4Cl(aq) until all had reacted to give a clear solution. This solution was filtered through cotton, reduced in volume under vacuum, and recrystallized with CH_2Cl_2/hexane (175 mg, 0.27 mmol, 77%). ^1H NMR (400 MHz, $C_{6D}6$): δ 0.81 (s, 9 H, C(CH_3)$_3$), 2.06 (s, 3 H, pzCH_3), 2.13 (s, 3 H, pzCH_3), 2.16 (s, 3 H, pzCH_3), 2.64 (s, 2 H, NCH_2), 2.81 (d, J = 1.7 Hz, 6 H, 3 H of pzCH_3, 3 H of OCH_3), 3.25 (s, 3 H, pzCH_3), 3.30 (s, 3 H, pzCH_3), 5.52 (s, 1 H, pz$H$), 5.53 (s, 1 H, pz$H$), 5.66 (s, 1 H, pz$H$), 6.76 (d, J = 8.8 Hz, 2 H, *Ph-m*), 7.59 (d, J = 8.8 Hz, 2 H, *Ph-o*). $^{13}C\{^1H\}$ NMR (400 MHz, C_6D_6): δ 12.3 (pzCH_3), 12.4 (pzCH_3), 12.7 (pzCH_3), 15.0 (pzCH_3), 15.7 (pzCH_3), 15.8 (pzCH_3), 26.6 (s, C(CH_3)$_3$), 32.4 (C(CH_3)$_3$), 54.7 (OCH_3), 56.3 (NCH_2), 84.5 (d, J = 39.6 Hz, Rh-CC-*p*-OMePh), 102.7 (d, J = 8.0 Hz, Rh−CC-*p*-OMePh), 107.5 (CH of pz), 107.9 (CH of pz), 108.3 (CH of pz), 113.0 (*p*-OM*ePh-o*), 121.8 (ipso *C* of *p*OMePh), 133.0 (*p*OM*ePh-m*), 142.8 (pzC_q), 143.3 (pzC_q), 144.3 (pzC_q), 152.2 (pzC_q), 152.3 (pzC_q), 154.6 (pzC_q), 158.2 (ipso COMe of Ph). IR (cm^{-1}) ν = 1974, 2031, 2156 (C≡C), 2237, 2532. Anal. Calcd for $C_{30}H_{40}BClN_7ORh\cdot1/3(CH_2Cl_2)$: C, 52.64; H, 5.92; N, 14.17. Found: C, 51.94; H, 6.36; N, 14.66.

Preparation of Tp′Rh(CNneopentyl)(C≡CC_6H_5)Cl (8a-Cl). A similar procedure to that for **7a-Cl** was employed (78% yield). ^1H NMR (400 MHz, C_6D_6): δ 0.80 (s, 9 H, C(CH_3)$_3$), 2.05 (s, 3 H, pzCH_3), 2.12 (s, 3 H, pzCH_3), 2.16 (s, 3 H, pzCH_3), 2.62 (s, 2 H, NCH_2), 2.77 (s, 3 H, pzCH_3), 2.80 (s, 3 H, pzCH_3), 3.26 (s, 3 H, pzCH_3), 5.51 (s, 1 H, pz$H$), 5.52 (s, 1 H, pz$H$), 5.65 (s, 1 H, pz$H$), 6.99 (t, J = 7.4 Hz, 1 H, *Ph-p*), 7.13 (t, J = 7.8 Hz, 2 H, *Ph-m*), 7.65 (dd, J = 8.1, 1.1 Hz, 2 H, *Ph-o*). $^{13}C\{^1H\}$ NMR (400 MHz; $CDCl_3$): 12.5 (pzCH_3), 12.7 (pzCH_3), 13.0 (pzCH_3), 14.6 (pzCH_3), 15.3 (pzCH_3), 15.4 (pzCH_3), 27.0 (s, C(CH_3)$_3$), 33.0 (C(CH_3)$_3$), 57.2 (NCH_2), 85.7 (d, J = 40.8 Hz, Rh-CCPh), 103.3 (d, J = 6.9 Hz, Rh−CCPh), 107.4 (CH of pz), 107.9 (CH of pz), 108.1 (CH of pz), 125.3 (ipso *C* of Ph), 127.7 (Ph-*m*), 128.2 (Ph-*p*), 131.6 (Ph-*o*), 143.5 (pzCq), 143.7 (pzCq), 144.0 (pzCq), 151.9 (pzCq), 152.3 (pzCq), 154.1 (pzCq). IR (cm^{-1}) ν = 1973, 2028, 2156 (C≡C), 2238, 2528. Anal. Calcd for $C_{29}H_{47}BClN_7Rh\cdot1/4(CH_2Cl_2)$: C, 53.64; H, 5.92; N, 15.71. Found: C, 54.14; H, 6.02; N, 15.05 (CH_2Cl_2 is observed in the NMR spectrum of **8a-Cl** at δ4.27, see p S-18 in Supporting Information).

Preparation of Tp′Rh(CNneopentyl)(C≡CC_6H_4-p-CF_3)Cl (9a-Cl). A similar procedure to that for **7a-Cl** was employed (63% yield), although a longer reaction time was required. ^1H NMR (400 MHz, C_6D_6): δ 0.79 (s, 9 H, C(CH_3)$_3$), 2.05 (s, 3 H, pzCH_3), 2.11 (s, 3 H, pzCH_3), 2.15 (s, 3 H, pzCH_3), 2.62 (s, 2 H, NCH_2), 2.70 (s, 3 H, pzCH_3), 2.78 (s, 3 H, pzCH_3), 3.20 (s, 3 H, pzCH_3), 5.54 (s, 1 H, pz$H$), 5.55 (s, 1 H, pz$H$), 5.65 (s, 1 H, pz$H$), 7.30 (d, J = 8.2 Hz, 2 H, *Ph-o*), 7.43 (d, J = 8.1 Hz, 2 H, *Ph-m*). $^{13}C\{^1H\}$ NMR (400 MHz, C_6D_6): δ 12.29 (pzCH3), 12.39 (pzCH_3), 12.7 (pzCH_3), 14.9 (pzCH_3), 15.6 (pzCH_3), 15.7 (pzCH_3), 26.5 (s, C(CH_3)$_3$), 32.4 (C(CH_3)$_3$), 56.3 (s, NCH_2), 94.28 (d, J = 41.7 Hz, Rh-CC-*p*-CF3Ph), 102.9 (d, J = 6.9 Hz, Rh−CC-*p*-CF_3Ph), 107.6 (CH of pz), 108.0 (CH of pz), 108.4 (CH of pz), 125.2 (ipso *C* of Ph), 125.2 (q, J_{C-F} = 3.4 Hz, CF_3), 128.1 (*p*-CF_3*Ph-m*, overlapping with C_6D_6) 132.0 (*p*-CF_3*Ph-o*), 143.1 (pzC_q), 143.5 (pzC_q), 144.6 (pzC_q), 152.1 (pzC_q), 152.2 (pzC_q), 154.5 (pzC_q). $^{19}F\{^1H\}$ NMR (C_6D_6): δ 1.20 (s). IR (cm^{-1}) ν = 1974, 2024, 2156 (C≡C), 2228, 2491. Anal. Calcd for $C_{30}H_{46}BClN_7Rh$: C, 51.34; H, 5.31; N, 13.97. Found: C, 51.83; H, 5.61; N, 13.69.

Preparation of Tp′Rh(CNneopentyl)(C≡CC_6H_4-p-OMe)H (7a). $LiEt_3BH$ (0.16 mmol) in THF was added to a solution of **7a-Cl** (10 mg, 0.016 mmol) dissolved in THF and stirred for 1 h. This sample was placed in an J-Young NMR tube and the solvent was removed in vacuo at room temperature. The resulting bright yellow residue was dissolved in C_6D_6. ^1H NMR (400 MHz, C_6D_6): δ −13.37 (d, J = 18.8 Hz, 1 H, Rh-*H*), 0.71 (s, 9 H, C(*CH*3)3), 2.15 (s, 3 H, pzCH_3), 2.19 (s, 3 H, pzCH_3), 2.30 (s, 3 H, pzCH_3), 2.34 (s, 3 H, pzCH_3), 2.53 (s, 2 H, NCH_2), 2.88 (s, 3 H, pzCH_3), 2.91 (s, 3 H, pzCH_3), 3.27 (s, 3 H, OCH_3), 5.52 (s, 1 H, pz*H*), 5.65 (s, 1 H, pz*H*), 5.80 (s, 1 H, pz*H*), 6.76 (d, J = 8.6 Hz, 2 H, *Ph-m*), 7.58 (d, J = 8.6 Hz, 2 H, *Ph-o*);

Preparation of Tp′Rh(CNneopentyl)(C≡CC_6H_5)H (8a). The synthesis of **8a** was identical to that of **7a** except that **8a-Cl** was used as a precursor. ^1H NMR (400 MHz, C_6D_6): δ −13.34 (d, J = 18.7 Hz, 1 H, Rh-*H*), 0.69 (s, 9 H, C(CH_3)$_3$), 2.15 (s, 3 H, pzCH_3), 2.19 (s, 3 H, pzCH_3), 2.29 (s, 3 H, pzCH_3), 2.32 (s, 3 H, pzCH_3), 2.51 (s, 2 H, NCH_2), 2.85 (s, 3 H, pzCH_3), 2.87 (s, 3 H, pzCH_3), 5.51 (s, 1 H, pz*H*), 5.65 (s, 1 H, pz*H*), 5.78 (s, 1 H, pz*H*), 6.96 (t, J = 7.2 Hz, 1 H, *Ph-p*), 7.06 (t, J = 7.6 Hz, 2 H, *Ph-m*), 7.50 (d, J = 7.1 Hz, 2 H, *Ph-o*).

Preparation of Tp′Rh(CNneopentyl)(C≡CC_6H_4-p-CF_3)H (9a). The synthesis of **9a** was identical to that of **7a** except that **9a-Cl** was used as a precursor. ^1H NMR (400 MHz, C_6D_6): δ −13.29 (d, J = 18.5 Hz, 1 H, Rh-*H*), 0.68 (s, 9 H, C(CH_3)$_3$), 2.14 (s, 3 H, pzCH_3), 2.18 (s, 3 H, pzCH_3), 2.28 (s, 3 H, pzCH_3), 2.30 (s, 3 H, pzCH_3), 2.51 (s, 2 H, NCH_2), 2.79 (s, 3 H, pzCH_3), 2.82 (s, 3 H, pzCH_3), 5.54 (s, 1 H, pz*H*), 5.65 (s, 1 H, pz*H*), 5.81 (s, 1 H, pz*H*), 7.30 (d, J = 8.0 Hz, 2 H, *Ph-o*), 7.42 (d, J = 8.0 Hz, 2 H, *Ph-m*).

Kinetics of Reductive Elimination Reactions of Terminal Alkynes from Complexes 2a−9a. Complexes **2a−9a** were synthesized by dissolving **1** (10 mg) in 0.5 mL of the desired terminal alkyne, followed by irradiation for 5−10 min at 10 °C. Volatiles were removed in vacuo, resulting in a yellowish residue which was dissolved in 0.6 mL of C_6D_6, followed by 2 mg of ferrocene added as an internal standard. This solution was placed into a J-Young NMR tube and

dx.doi.org/10.1021/ja301095r | J. Am. Chem. Soc. 2012, 134, 9276−9284

heated in a 100 °C oil bath. NMR spectra were recorded at regular intervals by ^{1}H NMR spectroscopy. Kinetic analysis was performed by integration of the decreasing hydride resonance relative to the signal for ferrocene. A first-order decay of the concentration of Tp′Rh(CNR)(C≡CR)H was plotted against time to give the rates of reductive elimination of the corresponding RC≡C−H, and Excel was used to determine the rate constant. Most reactions were followed for ∼3 half-lives.

Competition Experiments. A solution of **1** (15 mg, 0.025 mol) dissolved in the same volume ratio of benzene/pentane/mesitylene and a terminal alkyne (as indicated in Table 3) were placed in a J-Young NMR tube. Each sample was irradiated for 10 min at 10 °C. The solvent was immediately removed in vacuo at room temperature. The resulting yellow residue was dissolved in C_6D_6 and ^{1}H NMR spectra were collected. The ratio of C−H activation products was measured by integrating the hydride resonances in ^{1}H NMR spectrum. As many of the resonances were subject to partial overlap, a global spectral deconvolution routine (Mnova) was used to determine the contributions of each species. Errors are estimated at 15% (see Supporting Information for details). The integration ratio was used in eq 7 to calculate $k_{substrate}/k_{C6H6}$, which was then used to calculate bond strengths according to eq 8. Note that even if the error in the product ratio were 100% (i.e., off by a factor of 2), this corresponds to an error in the free energy $\Delta\Delta G^{\ddagger}$ of only $RT \ln(2) = 0.4$ kcal mol^{-1}, which is far less than the size of the data marker in Figure 5! The bond strength trends for terminal alkyne C−H activation are found to follow the same trend as seen with sp^2 and sp^3 C−H activation of normal hydrocarbons.

■ ASSOCIATED CONTENT

Supporting Information

Kinetic treatments for reductive elimination reactions and competition experiments, NMR spectra, DFT calculations, and details of the X-ray structure determinations of **2-Br**, **3a-Cl**, and **8-Cl** (CCDC deposition #865546−865548). This material is available free of charge via the Internet at http://pubs.acs.org.

■ AUTHOR INFORMATION

Corresponding Author

jones@chem.rochester.edu

Notes

The authors declare no competing financial interest.

■ ACKNOWLEDGMENTS

We thank the U.S. Department of Energy, Basic Energy Sciences (FG02-86ER13569) for their support of this work. G.C. thanks the Japanese Society for Promotion of Science for a visiting student fellowship. We are thankful to the Center for Integrated Research Computing (CIRC) at the University of Rochester for providing the necessary computing systems and personnel to enable the research presented in this manuscript.

■ REFERENCES

(1) See the special issue of *Chem. Rev.* **2010**, *110*(2), 575−1211, for 17 articles reviewing current aspects of C−H activation and functionalization.

(2) (a) Miura, M.; Tsuda, T.; Satoh, T.; Pivsa-Art, S.; Nomura, M. *J. Org. Chem.* **1998**, *63*, 5211. (b) Chatani, N.; Fukuyama, T.; Tatamidani, H.; KaKiuchi, F.; Murai, S. *J. Org. Chem.* **2000**, *65*, 4039. (c) Biele, M. D. K.; van Strijdonck, G. P. F.; de Vries, A. H. M.; Kamer, P. C. J.; de Vries, J. G.; van Leeuwen, P. W. N. M. *J. Am. Chem. Soc.* **2002**, *124*, 1586. (d) Ben-Ari, E.; Gandelman, M.; Rozenberg, H.; Shimon, L. J. W.; Milstein, D. *J. Am. Chem. Soc.* **2003**, *125*, 4714. (e) Jacob, J.; Jones, W. D. *J. Org. Chem.* **2003**, *68*, 3563. (f) Asaumi, T.; Matsuo, T.; Fukuyama, T.; Ie, Y.; KaKiuchi, F.; Chatani, N. *J. Org. Chem.* **2004**, *69*, 4433. (g) Zaitsev, V. G.; Daugulis, O. *J. Am. Chem. Soc.* **2005**, *127*, 4156. (h) Cai, G.; Fu, Y.; Li, Y.; Wan, X.; Shi, Z. *J. Am. Chem. Soc.* **2007**, *129*, 7666. (i) Li, L.; Jones, W. D. *J. Am. Chem. Soc.* **2007**, *129*, 10707. (j) Li, J.-J.; Mei, T.-S.; Yu, J.-Q. *Angew. Chem., Int. Ed.* **2008**, *47*, 6452. (k) Houlden, C. E.; Bailey, C. D.; Ford, J. G.; Gagné, M. R.; Lloyd-Jones, G. C.; Booker-Milburn, K. I. *J. Am. Chem. Soc.* **2008**, *130*, 10066.

(3) Zhang, Y.-H.; Shi, B.-F.; Yu, J.-Q. *J. Am. Chem. Soc.* **2009**, *131*, 5072.

(4) (a) Tsai, C.-C.; Shih, W.-C.; Fang, C.-H.; Li, C.-Y.; Ong, T.-G.; Yap, G. P. A. *J. Am. Chem. Soc.* **2010**, *132*, 11887. (b) Wang, X.; Leow, D.; Yu, J.-Q. *J. Am. Chem. Soc.* **2011**, *133*, 13864.

(5) Janowicz, A. H.; Bergman, R. G. *J. Am. Chem. Soc.* **1983**, *105*, 3929.

(6) Northcutt, T. O.; Wick, D. D.; Vetter, A. J.; Jones, W. D. *J. Am. Chem. Soc.* **2001**, *123*, 7257.

(7) Schock, L. E.; Marks, T. J. *J. Am. Chem. Soc.* **1988**, *110*, 7701.

(8) Bennett, J. L.; Wolczanski, P. T. *J. Am. Chem. Soc.* **1997**, *119*, 10696.

(9) Schaller, C. P.; Wolczanski, P. T. *Inorg. Chem.* **1993**, *32*, 131.

(10) Jones, W. D.; Feher, F. J. *Acc. Chem. Res.* **1989**, *22*, 91. Jones, W. D.; Feher, F. J. *J. Am. Chem. Soc.* **1984**, *106*, 1650.

(11) Jones, W. D.; Hessell, E. T. *J. Am. Chem. Soc.* **1993**, *115*, 554.

(12) Jones, W. D.; Wick, D. D. *Organometallics* **1999**, *18*, 495.

(13) Clot, E.; Besora, M.; Maseras, F.; Mégret, C.; Eisenstein, O.; Oelckers, B.; Perutz, R. N. *Chem. Commun.* **2003**, 490.

(14) Clot, E.; Mégret, C.; Eisenstein, O.; Perutz, R. N. *J. Am. Chem. Soc.* **2009**, *131*, 7817.

(15) Evans, M. E.; Burke, C. L.; Yaibuathes, S.; Clot, E.; Eisenstein, O.; Jones, W. D. *J. Am. Chem. Soc.* **2009**, *131*, 13464.

(16) Tanabe, T.; Brennessel, W. W.; Clot, E.; Eisenstein, O.; Jones, W. D. *Dalton Trans.* **2010**, 10495.

(17) Clot, E.; Mégret, C.; Eisenstein, O.; Perutz, R. N. *J. Am. Chem. Soc.* **2006**, *128*, 8350.

(18) Hessell, E. T.; Jones, W. D. *Organometallics* **1992**, *11*, 1496.

(19) Evans, M. E.; Burke, C. L.; Yaibuathes, S.; Clot, E.; Eisenstein, O.; Jones, W. D. *J. Am. Chem. Soc.* **2009**, *131*, 13564.

(20) Wick, D. D.; Reynolds, K. A.; Jones, W. D. *J. Am. Chem. Soc.* **1999**, *121*, 3974.

(21) Hydrocarbon C−H bond strengths are from Luo, Y.-R. *Comprehensive Handbook of Chemical Bond Energies*; CRC Press: Boca Raton, FL, 2007. Alkyne C−H bond strengths were calculated using B3LYP/6-31g**. Only phenylacetylene is reported in reference 21, with a large experimental error (133 ± 5 kcal mol^{-1}). For acetylene, D_{C-H} = 133.32(0.07) and for propyne, D_{C-H} = 130.2(3.0) are reported.

(22) Evans, M. E.; Li, T.; Vetter, A. J.; Rieth, R. D.; Jones, W. D. *J. Org. Chem.* **2009**, *74*, 6907.

(23) Clot, E.; Mégret, C.; Eisenstein, O.; Perutz, R. N. *J. Am. Chem. Soc.* **2006**, *128*, 8350.

(24) Alonso, F. J. G.; Höhn, A.; Wolf, J.; Otto, H.; Werner, H. *Angew. Chem., Int. Ed. Engl.* **1985**, *24*, 406.

(25) For reviews, see: Bruce, M. I. *Chem. Rev.* **1991**, *91*, 197. Katayama, H.; Ozawa, F. *Coord. Chem. Rev.* **2004**, *248*, 1703.

(26) Wick, D. D.; Jones, W. D. *Inorg. Chem.* **1997**, *36*, 2723.

(27) Peng, C.; Ayala, P. Y.; Schlegel, H. B.; Frisch, M. J. J. *Comput. Chem.* **1996**, *17*, 49.

(28) Becke, A. D. *J. Chem. Phys.* **1993**, *98*, 5648.

(29) Lee, C.; Yang, W.; Parr, R. G. *Phys. Rev. B* **1988**, *37*, 785.

(30) Zhao, Y.; Truhlar, D. G. *Theor. Chem. Acc.* **2008**, *120*, 215.

(31) Frisch, M. J.; et al. Gaussian09; Gaussian, Inc.: Wallingford, CT, 2009.

(32) Ehlers, A. W.; Bohme, M.; Dapprich, S.; Gobbi, A.; Hollwarth, A.; Jonas, V.; Köhler, K. F.; Stegmann, R.; Veldkamp, A.; Frenking, G. *Chem. Phys. Lett.* **1993**, *208*, 111.

(33) Hollwarth, A.; Bohme, M.; Dapprich, S.; Ehlers, A. W.; Gobbi, A.; Jonas, V.; Köhler, K. F.; Stegmann, R.; Veldkamp, A.; Frenking, G. *Chem. Phys. Lett.* **1993**, *208*, 237.

(34) Hehre, W. J.; Ditchfield, R.; Pople, J. A. *J. Chem. Phys.* **1972**, *56*, 2257.